

## Intestinal permeability and excretion into bile control the arrival of amlodipine into the systemic circulation after oral administration

Dragica Raušl, Nikoletta Fotaki, Ružica Zanoški, Maria Vertzoni, Biserka Cetina-Čižmek, M. Zahirul I. Khan and Christos Reppas

### Abstract

The objective of this study was to identify the factors controlling the arrival of amlodipine into the systemic circulation after oral administration in the fasting state. Dissolution data were collected with the rotating paddle and the flow-through apparatus. Caco-2 cell lines were used to assess the intestinal permeability characteristics. Actual in-vivo data were collected in 24 fasted healthy subjects after single-dose administration of the same amlodipine besylate tablet formulation used in the in-vitro dissolution studies. Regardless of the hydrodynamics, dissolution of amlodipine besylate tablets was rapid and complete in media simulating the contents of the upper gastrointestinal tract in the fasting state. Permeability of amlodipine through Caco-2 cell lines was lower than propranolol's and higher than ranitidine's, indicating that transport through the intestinal mucosa may be one process that limits the arrival into the systemic circulation. Indeed, the deconvoluted profile indicated that arrival into portal blood occurs at rates much slower than gastric emptying or dissolution rates. However, prediction of amlodipine's mean plasma profile after oral administration became possible only after additionally assuming excretion of amlodipine into the bile and a reasonable gastrointestinal residence time. Interestingly, in-vitro permeability data collected in this or in previous studies were inappropriate for simulating the mean actual plasma profile.

### Introduction

Amlodipine is a dihydropyridine calcium-channel blocker with alkaline characteristics ( $pK_a = 9.0$  (Mason et al 1989),  $\log P = 2.96$  (Caron et al 2004)) and an aqueous solubility of  $0.774 \text{ mg mL}^{-1}$  at  $37^\circ\text{C}$  (McDaid & Deasy 1996). Since it is administered at doses up to 10 mg, the dose-to-solubility ratio is few millilitres and, therefore, it is a highly soluble compound (Amidon et al 1995).

The absolute oral bioavailability of amlodipine besylate tablets ranges from 63 to 81% (Stopher et al 1988; Vincent et al 2000).  $T_{\max}$  values after oral administration are 6–9 h (e.g. Haria & Wagstaff 1995). The long  $T_{\max}$  values have been attributed to slow absorption or to sequestration in tissues after absorption (Stopher et al 1988). The terminal elimination half-life of amlodipine is 30–55 h (Meredith & Elliot 1992).

Although amlodipine undergoes extensive hepatic metabolism, the rates are low and first-pass or presystemic metabolism is minimal (Stopher et al 1988; Meredith & Elliott 1992; Haria & Wagstaff 1995). Therefore, potential restrictions to its arrival into the systemic circulation after oral administration could include slow dissolution of the dose intralumenally (it is known that highly soluble compounds may show dissolution-limited absorption (e.g. Dressman & Fleisher 1986; Yu 1999)) and slow transport via the intestinal mucosa. In addition, amlodipine is excreted in the faeces (Stopher et al 1988). It has not been clarified whether this is mostly due to problematic intestinal permeability or due to enterohepatic circulation of amlodipine itself or of a conjugate. Amlodipine has many characteristics of a compound that could be excreted into the bile (Roberts et al 2002), in that it has a molecular weight of 567.1, it has long plasma elimination half-life and it has a high apparent volume of distribution (Faulkner et al 1986; Stopher et al 1988).

PLIVA Research and Development Ltd., Prilaz baruna Filipovića 29, 10 000 Zagreb, Croatia

Dragica Raušl, Ružica Zanoški, Biserka Cetina-Čižmek, M. Zahirul I. Khan

Faculty of Pharmacy, Laboratory of Biopharmaceutics & Pharmacokinetics, National & Kapodistrian University of Athens, Panepistimiopolis, 15 771 Athens, Greece

Nikoletta Fotaki, Maria Vertzoni, Christos Reppas

**Correspondence:** C. Reppas, Faculty of Pharmacy, Laboratory of Biopharmaceutics and Pharmacokinetics, National & Kapodistrian University of Athens, Panepistimiopolis, 15 771 Zografou, Greece. E-mail: reppas@pharm.uoa.gr

The objective of this study was to clarify the importance of intraluminal dissolution, intestinal permeability and excretion into bile on the arrival of amlodipine into the systemic circulation after oral administration in the fasting state.

## Materials and Methods

### Materials

Amlodipine besylate pure substance was bought from Dr Reddy's Laboratories Ltd (Andhra Pradesh, India). Amlodipine besylate tablets were made by Pliva (Zagreb, Croatia) and contained 13.869 mg amlodipine besylate (equivalent to 10 mg amlodipine base). Amlodipine besylate working standard was also provided by Pliva (Zagreb, Croatia).

Propranolol hydrochloride and ranitidine hydrochloride were purchased from Sigma (Steinheim, Germany). Crude sodium taurocholate was also bought from Sigma, whereas soybean lecithin S 100 was a gift from Lipoid GmbH (Ludwingshafen, Germany). The content of crude sodium taurocholate in 3 $\alpha$ -hydroxy-bile salts was measured as 87.90% (Vertzoni et al 2004).

Caco-2 cells were obtained from European Collection of Cell Cultures (Salisbury, UK) at passage 43. Dulbecco's modified Eagles medium (DMEM) containing glucose (4500 mg mL<sup>-1</sup>) was purchased from Imunološki zavod (Zagreb, Croatia), fetal bovine serum (FBS), glutamax I, nonessential amino acids (NEAA), penicillin/streptomycin, Fungizone (amphotericin B) and trypsin-EDTA were obtained from Gibco Life Technologies (Paisley, UK). Rat tail collagen type I, Hanks balanced salt solution (HBSS), *N*-(2-hydroxyethyl) piperazine-*N'*-(2-ethanesulfonic acid) (HEPES), lucifer yellow (LY) and dimethyl sulfoxide (DMSO) were from Sigma (Steinheim, Germany). Polycarbonate Transwell inserts (24 mm diameter and 3  $\mu$ m pore size) were obtained from Costar (Cambridge, USA).

### In-vitro dissolution studies

A Distek dissolution system (model 2100B; North Brunswick, NJ, USA) equipped with a rotating paddle and an Erweka flow-through cell dissolution tester ( $\varnothing$  12 mm cells, model DFZ60; Heusenstamm, Germany) equipped with an Erweka Piston Pump (model HKP60; Heusenstamm, Germany) were used. Experiments were performed in triplicate at 37  $\pm$  0.5°C in simulated gastric fluid (SGF) (Dressman et al 1998) and in fasted-state simulated intestinal fluid (FaSSIF) (Vertzoni et al 2004).

When using the rotating paddle apparatus, the paddle was rotated at 100 rev min<sup>-1</sup> in 500 mL of medium. Four-millilitre samples (with volume replacement) were drawn using a Fortuna Optima syringe fitted with stainless tubing, and they were filtered through regenerated cellulose filters (pore size 0.45  $\mu$ m; Titan, Eatontown, NJ, USA).

When the flow-through apparatus was used, one tablet was placed on the holder and inserted into the cell with a

glass bead  $\varnothing$  5 mm on the bottom. One glass microfibre filter (pore size 0.7  $\mu$ m, MN-GF1,  $\varnothing$  25 mm; Macherey-Nagel, Duren, Germany) was inserted at the top of the cell for filtration. Flow rates were 6 mL min<sup>-1</sup> in SGF and 8 mL min<sup>-1</sup> in FaSSIF. These flow rates were chosen so that a compromise was achieved between net in-vivo flow rates and total volume of dissolution medium used within a physiologically relevant timeframe (Dressman et al 1998; Fotaki et al 2005a). At specified times, samples were collected in volumetric cylinders.

### In-vitro permeability studies

#### *Caco-2 cell culture*

The cells were grown at 37°C with 5% CO<sub>2</sub> and 90% relative humidity in DMEM supplemented with 10% FBS and 1% glutamax I, NEAA, penicillin (100 U mL<sup>-1</sup>)–streptomycin (100  $\mu$ g mL<sup>-1</sup>) and Fungizone (amphotericin B) in cell culture flasks. Cultures were split (1:3 to 1:6) approximately every 3–4 days when they reached 80–90% confluence using trypsin-EDTA. Culture medium was changed the day after passaging. For transport studies, cells at passages 57 and 59 were seeded onto collagen-coated 6-well polycarbonate Costar Transwell filter inserts, in prepared culture medium, at a density of 2 or 3  $\times$  10<sup>5</sup> per well. The filters were coated with rat-tail collagen type I according to manufacturer's instructions and were equilibrated with the medium for 2 h before start of the seeding. The medium was changed the day after the seeding and then three times per week. The Caco-2 cells were cultured on the filters for 21–23 days. The integrity of the cell monolayers was estimated by measuring the trans-epithelial electrical resistance (TEER) using a Milicell ERS meter (Millipore, USA) before the experiment. Only the cell monolayers with TEER values higher than 500  $\Omega$  cm<sup>2</sup> were used.

#### *Transport experiments and estimation of P<sub>app</sub>*

The apparent coefficient of permeability, P<sub>app</sub>, of amlodipine across Caco-2 cells was determined for both the apical-to-basolateral (AP-BL) and the basolateral-to-apical (BL-AP) direction at two pH values in the apical side, 6.5 and 7.4. The pH of transport medium in the basolateral side was always 7.4. In parallel with amlodipine, the AP-BL transport of propranolol and ranitidine was also studied. These compounds have been suggested as standards of high (propranolol) and low permeability (ranitidine) when using Caco-2 cell-lines (Food & Drug Administration 2000). The transport media were HBSS or HEPES (12 mM) buffers adjusted with NaOH to pH 6.5 or 7.4. The transport of amlodipine was studied at a concentration of 50  $\mu$ g mL<sup>-1</sup> (corresponding to the highest dose dissolved in 250 mL) whereas the transport of propranolol and ranitidine was studied at a concentration of 100  $\mu$ g mL<sup>-1</sup>. The integrity of the cell monolayers before the experiment was estimated by measuring the trans-epithelial electrical resistance (TEER), using a Milicell ERS meter (Millipore, USA), in the culture medium. Thereafter, the culture medium was removed and the monolayers were carefully washed twice with the transport medium and additionally incubated for 30 min. For

transport in the AP-BL direction the apical medium was removed and replaced with an equal volume of test solution or reference solutions. The transport in the BL-AP direction was performed by changing the basolateral medium with test substance. During the experiment, samples of 200  $\mu\text{L}$  were withdrawn from the acceptor compartments at predetermined time points (0, 30, 60, 90 and 120 min or 15, 30, 60, 90 and 120 min) and each sample was replaced with an equal amount of transport medium. From the donor compartments, 20- $\mu\text{L}$  samples were taken at 0 and 120 min. The TEER value was measured and the permeation of 0.1 mM lucifer yellow (LY) was measured at the end of the experiment to check the integrity of monolayers. During the experiment, the transport media, as well as the test and reference solutions, were kept at 37°C, and the plates were incubated at 37°C under moderate shaking conditions (55 rev min<sup>-1</sup>). The permeability coefficient, *P*, was calculated according to equation 1.

$$P = (dQ/dt) \times (C_0/A) \quad (1)$$

where *dQ/dt* is the linear rate of drug appearance in the acceptor compartment, *C*<sub>0</sub> is the initial drug concentration in the donor compartment and *A* is the surface area of the cell monolayer. All experiments were conducted at least in triplicate.

### In-vivo study

The study was conducted according to the current version of the Declaration of Helsinki (Edinburgh, Scotland, 2000) and in compliance to the current ICH-GCP Guidelines. Twenty-four healthy adults participated in the study after signing an informed written consent in duplicate. A copy of the consent form was given to the subjects and the other form was retained at the contract research organization that contracted the study.

Each fasted subject received a single tablet containing amlodipine besylate (equivalent to 10 mg of amlodipine) with a glass of water. Blood samples (8 mL) were collected at 0, 1, 3, 5, 6, 7, 8, 9, 10, 11, 12, 13, 14, 16, 24, 30, 36, 48 and 72 h following drug administration. Blood samples were collected in pre-labelled vacutainers containing EDTA as anticoagulant and centrifuged at 1891 g, 10°C, for 15 min. Plasma samples were kept at -60°C until analysis. Subjects remained fasted for 4 h after drug administration.

### Drug assays

#### *In-vitro* studies

For amlodipine, an HPLC-UV method was developed that involved the use of a Hypersil BDS C-18 column (150 × 4.6 mm, 5  $\mu\text{m}$ ) guarded with Hypersil BDS C-18 CPG precolumn. The mobile phase consisted of 0.05 M triethylaminophosphate aqueous solution (pH adjusted to 3.0 with phosphoric acid)-methanol-acetonitrile (50:35:15 v/v/v) at a flow rate of 1 mL min<sup>-1</sup>. Amlodipine was detected at a wavelength of 237 nm. In dissolution studies, the standard curves were linear (*R*<sup>2</sup> > 0.995, concentration

range 1.00–41.6  $\mu\text{g mL}^{-1}$ ), the detection limit was 0.20  $\mu\text{g mL}^{-1}$  and the quantification limit was 0.68  $\mu\text{g mL}^{-1}$ . In permeability studies, linear standard curves were also obtained (*R*<sup>2</sup> > 0.9990, concentration range 0.880–121  $\mu\text{g mL}^{-1}$ ), the detection limit was 0.56  $\mu\text{g mL}^{-1}$  and the quantification limit was 1.7  $\mu\text{g mL}^{-1}$ .

For propranolol, a validated HPLC-UV method with detection at 230 nm was developed. A Waters Symmetry C<sub>18</sub> column (150 × 4.6 mm, 5  $\mu\text{m}$  particle size) was equilibrated with a mobile phase composed of acetonitrile-trifluoroacetic acid (0.01%) (25:75 v/v). Its flow rate was 1 mL min<sup>-1</sup>. Calibration curves were linear in the concentration range of 0.1–136  $\mu\text{g mL}^{-1}$ . Limits of detection and quantification in plasma were 0.024 and 0.070  $\mu\text{g mL}^{-1}$ , respectively.

For ranitidine, a validated HPLC-UV method with detection at 320 nm was developed. A Waters Symmetry C<sub>18</sub> column (150 × 4.6 mm, 5  $\mu\text{m}$  particle size) was equilibrated with a mobile phase of acetonitrile-phosphate buffer (0.02 M, pH 7.0) (20:80 v/v). Its flow rate was 1 mL min<sup>-1</sup>. Calibration curves were linear in the concentration range of 2.5–104  $\mu\text{g mL}^{-1}$ . Limits of detection and quantification in plasma were 0.82 and 2.5  $\mu\text{g mL}^{-1}$ , respectively.

#### *In-vivo* study

The concentrations of amlodipine in human plasma were determined using a validated LC-MS-MS procedure. One millilitre of plasma was transferred into pre-labelled tubes, 50  $\mu\text{L}$  of sumatriptan solution (200 ng mL<sup>-1</sup>, internal standard, ISTD) were added to each tube and the resulting solution was vortexed for 1 min. Two millilitres of 0.1 M phosphate buffer (pH 6.0) were added and, after vortexing for 30 s, 50  $\mu\text{L}$  was injected. A Chromolith RP-18e column (50 × 4.6 mm) and a mobile phase consisting of acetonitrile-ammonium acetate buffer (2 mM, pH 3.8) (85:15 v/v) were used. Amlodipine and the ISTD were monitored by LC-MS-MS using the Multiple Reaction Monitoring (MRM) mode and the following mass transitions: 409.2 to 238.1 and 296.2 to 57.8, respectively, with dwell times of 500 ms for each of the transitions. The retention time for the drug and the ISTD were approximately 1.20 and 1.05 min, respectively. MacQuan software (version 1.6; PE Sciex, Foster City, CA) was used for evaluation of the chromatograms. Calibration curves using 8 standard concentrations (ranging from 0.255 ng mL<sup>-1</sup> to 10.011 ng mL<sup>-1</sup>) were constructed. The quantification limit was 0.255 ng mL<sup>-1</sup>. The inter-day precision of the quality control sample during the study was 5.3% (3.979 ng mL<sup>-1</sup>), 5.6% (7.958 ng mL<sup>-1</sup>) and 6.0% (0.716 ng mL<sup>-1</sup>).

#### Treatment of in-vivo data

Information for the input rates after oral administration could not be obtained directly from the oral data, because no compartmental model built in WinNonlin Professional (version 3.1; Pharsight Corporation) could be successfully fitted to the oral data.

A three-compartment disposition model was fitted (WinNonlin Professional, version 3.1; Pharsight

**Table 1** The values of the parameters estimated after fitting a three-compartment disposition model to mean intravenous data of amlodipine (Faulkner et al 1986)

Apparent volume of distribution of central compartment (L)	22.8 ± 0.4
Terminal elimination rate constant (h <sup>-1</sup> )	1.21 ± 0.05
Rate constant for the distribution from the central to the peripheral compartment 1 (h <sup>-1</sup> )	3.28 ± 0.08
Rate constant for the distribution from the central to the peripheral compartment 2 (h <sup>-1</sup> )	7.24 ± 0.16
Rate constant for the distribution from the peripheral 1 to the central compartment (h <sup>-1</sup> )	2.52 ± 0.14
Rate constant for the distribution from the peripheral 2 to the central compartment (h <sup>-1</sup> )	0.160 ± 0.005

Data are means ± s.e. of estimate.

Corporation) to mean intravenous data that have been reported previously (Faulkner et al 1986). The plasma concentration–time profile of amlodipine after intravenous administration was described by the following tri-exponential function:

$$C = 403.15e^{-12.64t} + 28.51e^{-1.75t} + 7.14e^{-0.02t} \quad (2)$$

The estimated parameters (Wagner 1993) are presented in Table 1.

Since amlodipine has a minimal first-pass effect (Haria & Wagstaff 1995), the deconvoluted mean oral profile (estimated using intravenous data as the weighting function (WinNonlin Professional, version 3.1; Pharsight Corporation)) represents the amount of amlodipine that arrives into the portal blood versus time profile. The first-order rate constant for the arrival of amlodipine into the portal blood was estimated, after fitting a first-order model to the cumulative amount absorbed vs time profile.

### Simulation of amlodipine's plasma profile after oral administration

The mean plasma profile after oral administration was simulated with Stella 5.0 (Cognitus Ltd, North Yorkshire, UK) using three approaches.

In the first approach, simulation was performed assuming that the gastrointestinal tract is a perfectly mixed tank from which the drug can be eliminated (excreted in locations of the distal colon where absorption is not possible) and be transported into the portal blood. Elimination from the gastrointestinal lumen was simulated as a first-order process assuming 18 h as total gastrointestinal residence time (e.g. Macheras et al 1995). Arrival into the portal blood was assumed to also follow first-order kinetics with the rate constant, *k*, estimated from the deconvoluted oral profile:

$$dM/dt = k \times M \quad (3)$$

where *M* is the amount of amlodipine reaching the portal blood. Upon arrival to the portal blood, no further

restrictions for reaching the systemic circulation were assumed whereas the disposition parameters were obtained from Table 1.

In the second approach, simulation was performed by including biliary excretion in the model used in the first approach. Enterohepatic circulation was simulated after consideration of the gallbladder emptying pattern, and after characterization of the reversible first-order drug transport from the liver to the systemic circulation and the non-reversible first-order drug transport from the liver to the gallbladder. The gallbladder was assumed to empty into the duodenum at 5, 11, 24, 29, 35, 48, 53, 59 and 72 h post dosing (i.e. at times of meal intakes). At these times, the gallbladder was assumed to be totally emptied within 1 h (e.g. Macheras et al 1995) and the emptying process was assumed to be of first order (i.e. the emptying rate constant was assumed to be 3 h<sup>-1</sup>). Characterization of the two first-order processes related to enterohepatic circulation was possible by fitting the model shown in Figure 1 to previously published mean intravenous data (Faulkner et al 1986) (WinNonlin Professional, version 3.1; Pharsight Corporation). Numerical solution of the differential equations that describe the system in Figure 1 was possible by using as initial values the parameters presented in Table 1 and the first-order rate constant estimated after the deconvolution of the oral data.

In the third approach, the arrival of amlodipine into the portal blood was simulated by using the model described in the second approach with one modification: the gastrointestinal lumen was assumed to consist of five discrete compartments representing the stomach, the

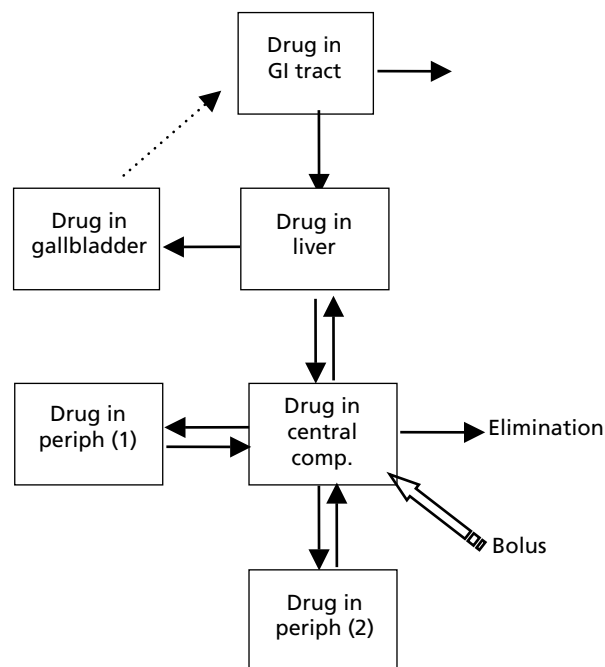


**Figure 1** Schematic representation of the model that was fitted to mean intravenous data of amlodipine (Faulkner et al 1986) for estimating the characteristics of the non-reversible transport from the liver to the gallbladder and the reversible transport from the liver to the central compartment.

duodenum, the jejunum, the ileum and the colon with the following characteristics. Intra-gastric dissolution was considered instantaneous and the gastric emptying rate constant was assumed to be  $2.8 \text{ h}^{-1}$  (Nicolaidis et al 2001). Residence times in duodenum, jejunum and ileum were assumed to be 0.5, 1 and 2 h, respectively, and transit of the liquid content was assumed to occur according to first-order kinetics (Yu et al 1996). Colonic residence time was assumed to be 14 h (e.g. Macheras et al 1995). The rate of appearance in portal blood was estimated using equation 3 and the rate constant was estimated using WinNonlin Professional, version 3.1 (Pharsight Corporation) (Table 3). In addition, the rate of appearance into the portal blood was estimated using the following equation:

$$dM/dt = [(P \times SA)/V] \times M \quad (4)$$

P was assumed to be equal to the value obtained from the Caco-2 experiments (this study) and equal to the value estimated previously from parallel artificial membrane permeability study (PAMPA) experiments (Caron et al 2004). The intestinal surface area available for transport (SA) and the volume of fluid from which the drug is taken up by the intestinal mucosa (V) were estimated as described recently (Fotaki et al 2005b) and assuming that the intestinal fluid volume at any given time during the first 3.5 h in the intestine is 150 mL and for times longer than 3.5 h is 50 mL (Badley et al 1993; Schiller et al 2005). It is noteworthy that estimation of intraluminal volumes and effective intestinal surface area (needed when simulation of the arrival into the portal blood involves the use of permeability coefficients) is greatly facilitated by a compartmental consideration of the gastrointestinal lumen.

### Profile comparisons

Comparison of simulated plasma profiles with the actual mean oral data set (reference profile) was performed with the use of the difference factor estimated using areas,  $f_{1,area}$  (Vertzoni et al 2003), and, therefore, the percent difference of a simulated profile from the mean oral profile was estimated ( $\%f_{1,area}$ ). Evaluation of  $f_{1,area}$  was considered up to 72 h.

## Results

### Dissolution data

As shown in Figure 2, dissolution data indicated rapid and complete dissolution of amlodipine besylate tablets in both SGF and FaSSIF, regardless of the hydrodynamics. The data obtained in SGF using the paddle apparatus suggested the possibility for degradation of the drug in this medium. Degradation in SGF could probably be related to the presence of sodium lauryl sulfate. This surfactant hydrolyses in solutions of  $\text{pH} < 4$  (Food Chemical Codex, 1981) leading to inconsistent medium composition. Also, artificial surfactants can interfere with salt formation rates of weak bases and, thus, dissolution can be affected in an artefactual way as has been

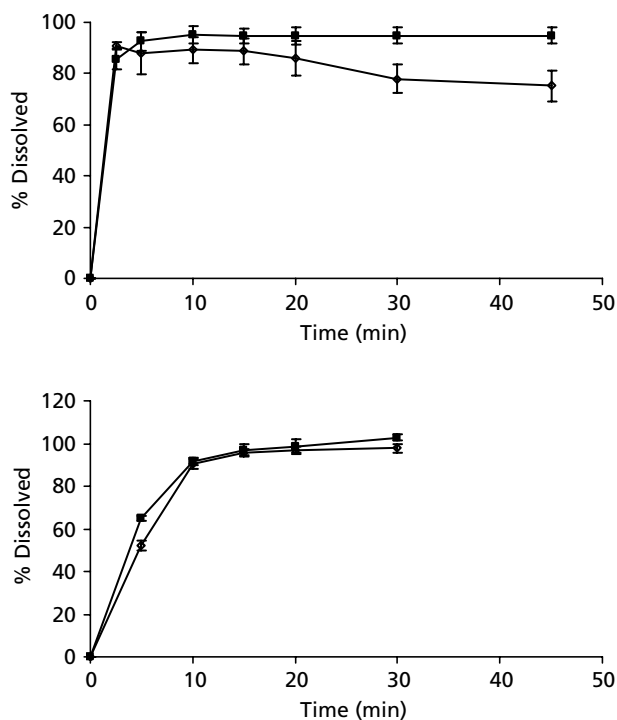


**Figure 2** Cumulative % dissolved vs time data sets for amlodipine besylate tablets using the rotating paddle apparatus (upper graphs) and the flow-through apparatus (lower graphs) in SGF (diamonds) and in FaSSIF (squares). Data are means  $\pm$  s.d.,  $n = 3$ .

observed with other alkaline compounds (Chen et al 2003). However, since the degradation process proved to be very slow (a relevant stability study indicated a degradation half-life of 32.6 h – data not shown), and a similar behaviour was not observed with the flow-through apparatus (Figure 2), it is also possible that amlodipine besylate in the vessel of the paddle apparatus undergoes a change of the crystal structure (e.g. <http://ep.espacenet.com>, abstract of WO03043635). Unlike the rotating paddle apparatus, with the flow-through apparatus 100% dissolution is measured, whereas filtration takes place immediately upon dissolution.

### Permeability data

Estimated apparent permeability coefficients for amlodipine, propranolol and ranitidine are presented in Table 2. Based on the values of the apparent permeability coefficients of propranolol (highly permeability marker), ranitidine (low permeability marker) and amlodipine at apical pH 6.5, amlodipine has low permeability characteristics (Food & Drug Administration 2000). This is in agreement with Yee (1997) who has classified amlodipine as a moderately permeable drug with pH-dependent transport. The apparent permeability coefficient increased more than 4 times (from  $1.75 \pm 0.27 \times 10^{-6} \text{ cm s}^{-1}$  to  $7.43 \pm 0.87 \times 10^{-6} \text{ cm s}^{-1}$ ) in the apical-to-basolateral direction (AP-BL) when the apical pH was increased from pH 6.5 to 7.4. In the basolateral-

**Table 2** Permeability coefficients ( $\times 10^6 \text{ cm s}^{-1}$ ) estimated using Caco-2 cell lines for the apical-to-basolateral transport (AP-BL) of propranolol, ranitidine and amlodipine and for the basolateral-to-apical transport (BL-AP) of amlodipine using two different apical pH values

pH		Propranolol AP-BL	Ranitidine AP-BL	Amlodipine	
AP	BL			AP-BL	BL-AP
6.5	7.4	7.32 $\pm$ 0.51	0.25 $\pm$ 0.01	1.75 $\pm$ 0.27	18.78 $\pm$ 1.13
7.4	7.4	14.22 $\pm$ 2.05	0.45 $\pm$ 0.02	7.43 $\pm$ 0.87	7.14 $\pm$ 0.60

Data are means  $\pm$  s.d.

to-apical direction (BL-AP), transport was decreased significantly when the pH in the apical side increased from 6.5 to 7.4 (from  $18.8 \pm 1.13 \times 10^{-6} \text{ cm s}^{-1}$  to  $7.14 \pm 0.60 \times 10^{-6} \text{ cm s}^{-1}$ ). Experiments using Caco-2 cell lines are often conducted using a pH gradient in which the pH on the apical side is 6.5 (Yamashita et al 2000). We therefore determined the rates of pH-dependent passive efflux under this pH gradient and compared them with the rates obtained when the pH on both sides was equal (pH 7.4/7.4). At equal pH values the bidirectional permeabilities of amlodipine were not significantly different. In contrast, when a pH gradient was present (apical 6.5, basolateral 7.4) the AP-BL transport was lower than the BL-AP transport rates, revealing that the observed efflux for amlodipine is indeed passive efflux. Similar passive efflux across Caco-2 cell monolayers has been also observed with other weakly basic compounds (Neuhoff et al 2003). However, based on the data with propranolol and ranitidine (Table 2), increasing the pH of the apical side, the  $P_{\text{app}}$  value for either propranolol or ranitidine (both bases with  $\text{pK}_{\text{as}}$  9.5 and 8.2, respectively) (Yoshida & Topliss 2000) was affected much less than the  $P_{\text{app}}$  of amlodipine, presumably due to the lower lipophilicity of propranolol ( $\log D_{6.5} = -0.02$ ) or ranitidine ( $\log D_{6.5} = -1.44$ ) than the lipophilicity of amlodipine. Cationic amlodipine is more lipophilic than would be expected from its structure partly due to intramolecular interaction (mostly formation of hydrogen bonds);  $\log D_{6.5}$  and  $\log D_{7.4}$  have been reported to be 0.78 and 1.55, respectively (Yoshida & Topliss 2000; Caron et al 2004).

### In-vivo data

In every individual profile, a second peak was observed close to the time of consumption of the first meal after dosing (individual data not shown).

The mean  $\pm$  s.d. values for  $\text{AUC}_{0-72}$  and  $C_{\text{max}}$  were  $163 \text{ ng mL}^{-1} \text{ h}$  and  $4.3 \pm 0.9 \text{ ng mL}^{-1}$ , respectively. Median (range) values for  $T_{\text{max}}$  were 7.0 (5.0–12.0) h. These data are in agreement with previously reported oral data of amlodipine tablets (Faulkner et al 1986; Vincent et al 2000).

The cumulative arrival into the portal blood versus time profile estimated after deconvolution of the oral data and the best fitted line ( $R^2 = 0.985$ ) are shown in Figure 3. The estimated first-order absorption rate

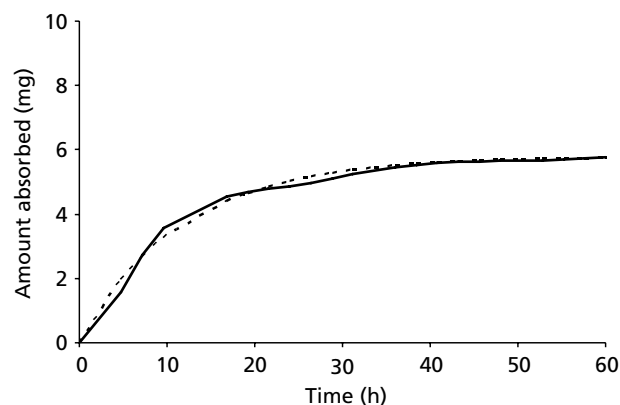


**Figure 3** Cumulative amount of amlodipine in the portal blood versus time plot after oral administration of an amlodipine besylate tablet formulation (equivalent to 10 mg amlodipine) in the fasted state that was estimated after deconvolution of the plasma data (continuous line) and the best fitted line according to the first-order model (dotted line).

constant was  $0.085 \pm 0.004 \text{ h}^{-1}$ . This value confirms that neither intraluminal dissolution nor gastric emptying affect the appearance rates of amlodipine in the portal blood because both processes take place at much faster rates than the rates corresponding to the estimated rate constant. Therefore, arrival into the portal blood seems to be limited by the transport via the intestinal mucosa.

Both actual and fitted profiles of Figure 3 plateaued at about 5.8 mg. This value corresponds to an oral bioavailability of 58%, which deviates from the generally accepted range of bioavailability (63–81%; Stopher et al 1988; Vincent et al 2000). Deviation should be attributed to the fact that the deconvolution was performed using mean oral and intravenous data collected from different sets of subjects.

### Predicted versus actual plasma data

Figure 4 shows the mean  $\pm$  s.d. actual plasma data after oral administration of an amlodipine besylate tablet to 24 subjects and the simulated profile constructed with the model, shown at the top of the figure. The difference of the simulated profile from the mean actual profile was 27.7%. Moreover, although the simulated profile predicts the  $C_{\text{max}}$  value of the mean actual data set ( $3.92 \text{ ng mL}^{-1}$  vs  $3.98 \text{ ng mL}^{-1}$ , respectively), it underestimates the  $T_{\text{max}}$  value of the mean actual data sets (1.4 h vs 7.0 h, respectively) and, therefore, it overestimates the rates of arrival at the systemic circulation.

Pharmacokinetic parameters estimated after fitting the model shown in Figure 1 to mean intravenous data (Faulkner et al 1986) are presented in Table 3. It is interesting to note that the disposition parameters are almost identical to those estimated assuming a classical three-compartment model without the assumption of enterohepatic circulation (Table 3 vs Table 1). Also, the rate constant for the transport of amlodipine from the gastrointestinal lumen to the liver (Table 3) is similar to the rate constant estimated from the cumulative deconvoluted profile (Figure 3).

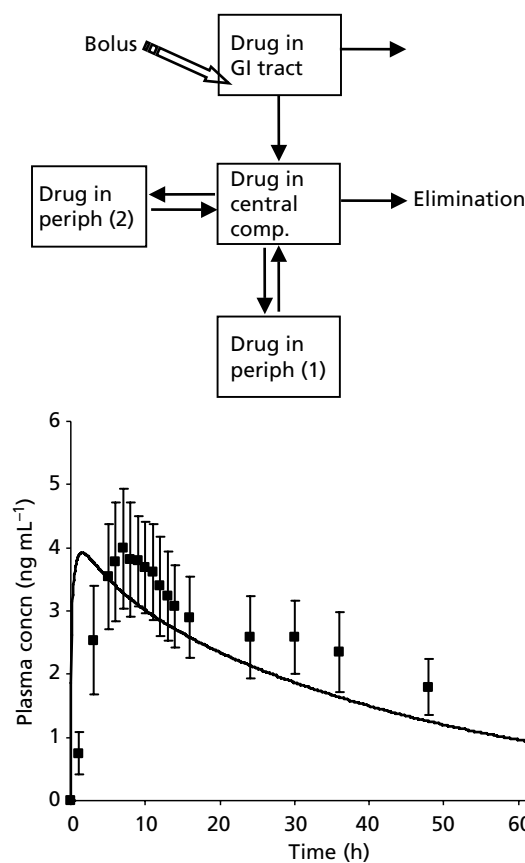


**Figure 4** Schematic representation of the model (top) used to obtain the simulated plasma concentration vs time plot (bottom) and the mean  $\pm$  s.d. actual data points from 24 healthy subjects. Model parameters were obtained from Table 1. Also, the elimination from the gastrointestinal lumen was assumed to take place according to first-order kinetics and the total residence time was 18 h, whereas the transport from the gastrointestinal tract into the central compartment was simulated using the rate constant estimated from the deconvoluted profile (Figure 3).

Figure 5 shows the mean  $\pm$  s.d. actual plasma data after oral administration of an amlodipine besylate tablet to 24 subjects and the simulated profile constructed by using the model, shown at the top of Figure 5. In contrast to Figure 4, the difference of the simulated profile to the mean actual profile was much less (8%). Moreover, the simulated profile predicted both the  $C_{\max}$  and the  $T_{\max}$  values of the mean actual data set ( $3.98 \text{ ng mL}^{-1}$  vs  $3.98 \text{ ng mL}^{-1}$ , and  $6.2 \text{ h}$  vs  $7.0 \text{ h}$ , respectively).

Figure 6 shows the mean  $\pm$  s.d. actual plasma data after oral administration of an amlodipine besylate tablet to 24 subjects and three simulated profiles constructed by assuming that the transport into the portal blood is governed by the permeability coefficient estimated from Caco-2 experiments ( $1.75 \times 10^{-6} \text{ cm s}^{-1}$ , Table 2), the permeability coefficient estimated from PAMPA experiments ( $1023 \times 10^{-6} \text{ cm s}^{-1}$ , Caron et al 2004) and from the first-order rate constant shown in Figure 3 ( $0.1 \text{ h}^{-1}$ ). It can be concluded that neither Caco-2 data nor PAMPA data are useful for predicting the plasma profile (the difference

**Table 3** Values of the parameters estimated after fitting the model shown in Figure 1 to mean intravenous data of amlodipine (Faulkner et al 1986)

Terminal elimination rate constant ( $\text{h}^{-1}$ )	$1.00 \pm 0.01$
Rate constant for the distribution from the central to the peripheral compartment 1 ( $\text{h}^{-1}$ )	$3.280 \pm 0.002$
Rate constant for the distribution from the central to the peripheral compartment 2 ( $\text{h}^{-1}$ )	$7.200 \pm 0.004$
Rate constant for the distribution from the peripheral 1 to the central compartment ( $\text{h}^{-1}$ )	$2.520 \pm 0.001$
Rate constant for the distribution from the peripheral 2 to the central compartment ( $\text{h}^{-1}$ )	$0.1600 \pm 0.0001$
Rate constant for the transport of drug from the central compartment to the liver ( $\text{h}^{-1}$ )	$0.100 \pm 0.001$
Rate constant for the transport of drug from the liver to the central compartment ( $\text{h}^{-1}$ )	$0.41 \pm 0.01$
Rate constant for the transport of drug to the storage compartment (gall bladder) ( $\text{h}^{-1}$ )	$0.05 \pm 0.01$
Rate constant for the transport of drug from the GI lumen to the liver ( $\text{h}^{-1}$ )	$0.12 \pm 0.02$

Data are means  $\pm$  s.e. of estimate.

between the corresponding simulated profiles and the mean actual profile was 85.6% and 101.7%, respectively). Compared with Figure 5, the first-order rate constant led to slightly worse prediction of the mean actual profile ( $f_{1,area} = 0.09$  in Figure 6 vs  $f_{1,area} = 0.08$  in Figure 5) and slightly worse prediction of the  $C_{\max}$  and  $T_{\max}$  mean actual data (the predicted profile in Figure 6 had  $C_{\max}$   $4.25 \text{ ng mL}^{-1}$  and  $T_{\max}$   $6.0 \text{ h}$ ). This should be attributed to the increased number of parameters used for simulating the intraluminal disposition of amlodipine in Figure 6. Even so, however, the first-order rate led to adequate prediction of the mean actual plasma data. It is interesting to note that by using the following equation (after combining equations 3 and 4):

$$P = (k \times V) / SA \quad (5)$$

and the geometric characteristics of the small intestine (Yee 1997; Fotaki et al 2005b), the permeability coefficient corresponding to the value of the rate constant for the transport of amlodipine from the intestine to the liver (Table 3) is estimated to be  $0.25 \times 10^{-4} \text{ cm s}^{-1}$ . According to Fagerholm et al (1996), compounds with  $0.1 \times 10^{-4} \text{ cm s}^{-1} < P < 0.7 \times 10^{-4} \text{ cm s}^{-1}$  in man should be classified as having an intermediate extent of absorption (i.e. 30–90%). Indeed, this range of values includes the values of the extent of absorption that have been reported in literature (63%, Stopher et al 1988; 81%, Vincent et al 2000) and in this study (58%, Figure 3).

## Discussion

This study showed that intestinal permeability and enterohepatic circulation of amlodipine are the major determinants of its arrival into the systemic circulation.

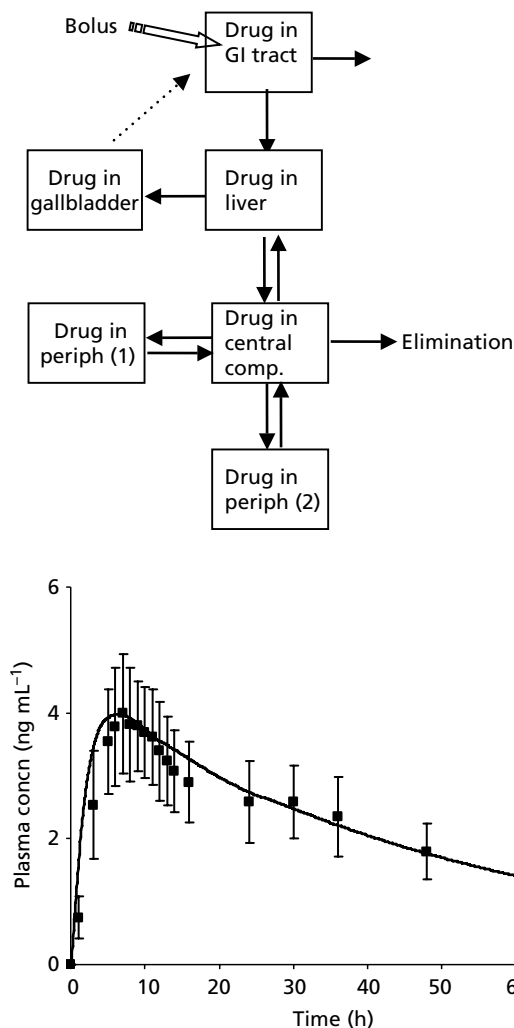


**Figure 5** Schematic representation of the model (top) used to obtain the simulated plasma concentration vs time plot (bottom) and the mean  $\pm$  s.d. actual data points from 24 healthy subjects. Model parameters were obtained from Table 3. Also, the elimination from the gastrointestinal lumen was assumed to take place according to first-order kinetics and the total residence time was 18 h, the transport from the gastrointestinal tract into the central compartment was simulated using the rate constant estimated from the deconvoluted profile (Figure 3) and the gallbladder was assumed to empty within one hour upon meal intake (please see Methods).

Although speculations on the enterohepatic circulation of amlodipine have been made in a previous study (Stopher et al 1988), its importance in relation to the reduced permeability characteristics had not been studied. Based on Figures 5 and 6, enterohepatic circulation decreases the rate of arrival into the systemic circulation.

In regard to the permeability of amlodipine, data collected from Caco-2 and PAMPA experiments led to vast underestimation and overestimation of the plasma levels, respectively (Figure 6) and, therefore, they were for different reasons inappropriate for predicting the plasma levels after oral administration.

Artificial membrane and Caco-2 cell lines are different in that the former mimics the passive transcellular route of drug transport only, while Caco-2 lines to a varying degree mimic additional transport mechanisms. Therefore, the correlation between artificial membrane permeability and Caco-2 permeability is not expected to be ideal (Kansy et al 1998; Zhu et al 2002). Kerns et al (2004) showed that compounds that have higher PAMPA permeability than cell monolayer permeability are subject to secretory mechanisms, including efflux and pH-gradient secretory enhancement of passive diffusion by bases. Indeed, the Caco-2 data collected in this study showed that the efflux ratio for amlodipine was considerably greater than 1.0 when the commonly used pH gradient of 6.5 (apical) and 7.4 (basolateral) was used (Table 2). The efflux ratio was approximately 1.0, however, in the absence of a pH gradient (i.e. amlodipine is not actively transported under the applied experimental conditions). This is in agreement with previous indications that amlodipine may not be a substrate for P-glycoprotein transport (Vincent et al 2000). Presumably, the pH-dependent permeability of amlodipine is, at least partly, the reason for the underestimation of the bioavailability of amlodipine by quantitative structure-activity relationship models that are based on the distribution coefficient at pH 6.5 (e.g. Yoshida & Topliss 2000).

One reason for the vast underestimation of the human plasma profile when using the Caco-2 cell data might be related to the underestimation of permeability coefficients of slowly (passively) transported drugs or the underestimation of the carrier-mediated transport rates when using this in-vitro set-up (Lennernaes et al 1996).

Finally, it could be argued that the failure of Caco-2 data to predict the human plasma profile is related to the well-known high inter-laboratory variability of such data. Although there are no published Caco-2 data for amlodipine and a previously estimated permeability coefficient for ranitidine using Caco-2 cell lines ( $0.1 \times 10^{-6} \text{ cm s}^{-1}$  (Gan et al 1993)) is similar to the value estimated in this study (Table 2), for propranolol, various values for the permeability coefficient have been reported and some of them (e.g.  $87.4 \times 10^{-6} \text{ cm s}^{-1}$  (Miret et al 2004)) deviate substantially from the value estimated in this study (Table 2). If human permeability data are not available, in-vitro permeability data for direct prediction of the in-vivo plasma profile could be used but only if they are confirmed by data using another in-vitro or in-situ technique (e.g. Fotaki et al 2005b).

## Conclusions

This study showed that intestinal permeability restricts the absorption of amlodipine after oral administration. However, the arrival of amlodipine into the systemic circulation is additionally limited by the excretion of amlodipine (or of a conjugate of amlodipine) into the bile. In-vitro Caco-2 cell or PAMPA data were not useful for the assessment of the plasma profile of amlodipine after single oral administration.



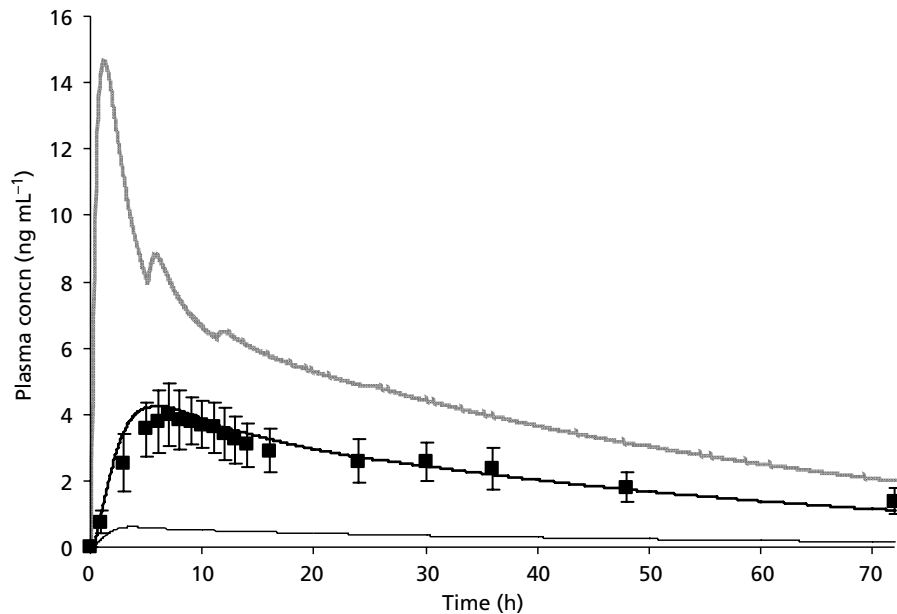
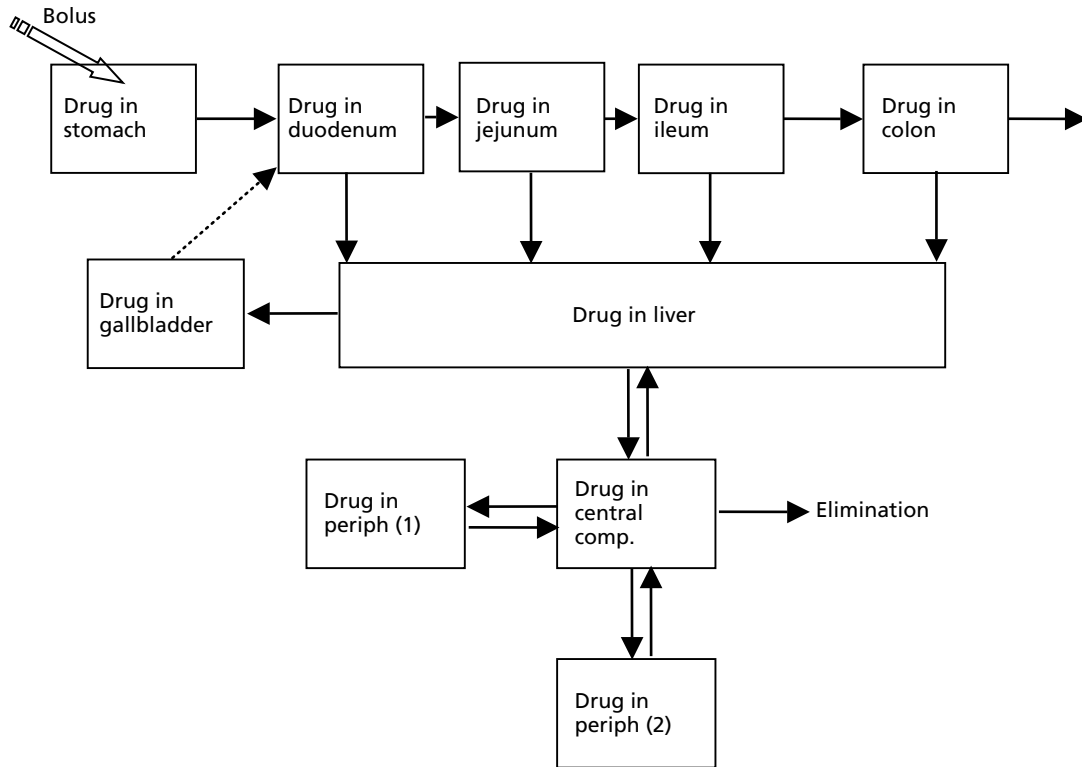


**Figure 6** Schematic representation of the model (top) used to obtain the simulated plasma concentration vs time plots (bottom) and the mean  $\pm$  s.d. actual data points from 24 healthy subjects. Simulated profiles were constructed using the permeability coefficient estimated from PAMPA experiments (Caron et al 2004; bold grey line) using the permeability coefficient estimated from Caco-2 experiments (Table 2; thin black line) and using the first-order absorption rate constant estimated from the deconvoluted profile (Figure 3; bold black line). Intraluminal disposition model characteristics are described in Methods. The rest of the model parameters were as described in Figure 5.

## References

- Amidon, G. L., Lennernäs, H., Shah, V. P., Crison, J. R. (1995) A theoretical basis for a biopharmaceutical drug classification: the correlation of *in vitro* drug product dissolution and *in vivo* bioavailability. *Pharm. Res.* **12**: 413–420
- Badley, A. D., Camilleri, M., O'Connor, M. K. (1993) Noninvasive measurement of human ascending colon volume. *Nucl. Med. Commun.* **14**: 485–489
- Caron, G., Ermondi, G., Damiano, A., Novaroli, L., Tsinman, O., Ruell, J. A., Avdeef, A. (2004) Ionization, lipophilicity, and molecular modelling to investigate permeability and other biological properties of amlodipine. *Bioorganic Med. Chem.* **12**: 6107–6118
- Chen, L., Wesley, J., Bhattachar, S., Ruiz, B., Bahash, K., Babu, S. (2003) Dissolution behavior of a poorly water soluble compound in the presence of Tween 80. *Pharm. Res.* **20**: 797–801
- Dressman, J. B., Fleisher, D. (1986) Mixing tank model for predicting dissolution rate control of oral absorption. *J. Pharm. Sci.* **75**: 109–116
- Dressman, J. B., Amidon, G. L., Reppas, C., Shah, V. P. (1998) Dissolution testing as a prognostic tool for oral drug absorption: immediate release dosage forms. *Pharm. Res.* **15**: 11–22
- Fagerholm, U., Johansson, M., Lennernas, H. (1996) Comparison between permeability coefficients in rat and human jejunum. *Pharm. Res.* **13**: 1336–1342
- Faulkner, J. K., McGibney, D., Chasseaud, L. F., Perry, J. L., Taylor, I. W. (1986) The pharmacokinetics of amlodipine in healthy volunteers after single intravenous and oral doses and after 14 repeated oral doses given once daily. *Br. J. Clin. Pharmacol.* **22**: 21–25
- Food Chemicals Codex* (1981) 3rd Edition, National Academy Press, Washington
- Food and Drug Administration (2000) CDER, Guidance for Industry. Waiver of *in vivo* bioavailability and bioequivalence studies for immediate-release solid oral dosage forms based on a biopharmaceutics classification system, August 2000.
- Fotaki, N., Symillides, M., Reppas, C. (2005a) *In vitro* vs. canine data for predicting input profiles of isosorbide-5-mononitrate from oral extended release products on a confidence interval basis. *Eur. J. Pharm. Sci.* **24**: 115–122
- Fotaki, N., Symillides, M., Reppas, C. (2005b) *In vitro* vs. canine data for predicting blood levels of l-sulpiride – a low permeability compound – in the fed state. *Eur. J. Pharm. Sci.* **26**: 324–333
- Gan, L. S., Hsyu, P. H., Pritchard, J. F., Thakker, D. (1993) Mechanism of intestinal absorption of ranitidine and ondansetron: transport across Caco-2 cell monolayers. *Pharm. Res.* **10**: 1722–1725
- Haria, M., Wagstaff, A. J. (1995) Amlodipine. A reappraisal of its pharmacological properties and therapeutic use in cardiovascular disease. *Drugs* **50**: 560–586
- Kansy, M., Senner, F., Gubernator, K. (1998) Physicochemical high throughput screening: parallel artificial membrane permeation assay in the description of passive absorption processes. *J. Med. Chem.* **41**: 1007–1010
- Kerns, E. H., Di, L., Petusky, S., Farris, M., Ley, R., Jupp, P. (2004) Combined application of parallel artificial membrane permeability assay and Caco-2 permeability assays in drug discovery. *J. Pharm. Sci.* **93**: 1440–1453
- Lennernaes, H., Palm, K., Fagerholm, U., Artursson, P. (1996) Comparison between active and passive drug transport in human intestinal epithelial (Caco-2) cells *in vitro* and human jejunum *in vivo*. *Int. J. Pharm.* **127**: 103–107
- Macheras, P., Reppas, C., Dressman, J. B. (1995) *Biopharmaceutics of orally administered drugs*. Ellis Horwood Series in Pharmaceutical Technology, ISBN 0-13-108093-8, London, UK
- Mason, R. P., Campbell, S. F., Wang, S. D., Herbette, L. G. (1989) Comparison of location and binding for the positively charged 1,4-dihydropyridine calcium channel antagonist amlodipine with uncharged drugs of this class in cardiac membranes. *Mol. Pharmacol.* **36**: 634–640
- McDaid, D. M., Deasy, P. B. (1996) Formulation development of a transdermal drug delivery system for amlodipine base. *Int. J. Pharm.* **133**: 71–83
- Meredith, P. A., Elliott, H. L. (1992) Clinical pharmacokinetics of amlodipine. *Clin. Pharmacokinet.* **22**: 22–31
- Miret, S., Abrahamse, L., Groene, E. (2004) Comparison of *in vitro* models for the prediction of compound absorption across the human intestinal mucosa. *J. Biomol. Screening* **9**: 598–606
- Neuhoff, S., Ungell, A. L., Zamora, I., Artursson, P. (2003) pH-dependent bidirectional transport of weakly basic drugs across Caco-2 monolayers: implications for drug-drug interactions. *Pharm. Res.* **20**: 1141–1148
- Nicolaides, E., Symillides, M., Dressman, J. B., Reppas, C. (2001) Biorelevant dissolution testing to predict the plasma profile of lipophilic drugs after oral administration. *Pharm. Res.* **18**: 380–388
- Roberts, M. S., Magnusson, B. M., Burczynski, F. J., Weiss, M. (2002) Enterohepatic circulation: physiological, pharmacokinetic and clinical implications. *Clin. Pharmacokinet.* **41**: 751–790
- Schiller, C., Frohlich, C. P., Giessmann, T., Siegmund, W., Monnikes, H., Hosten, N., Weitschies, W. (2005) Intestinal fluid volumes and transit of dosage forms as assessed by magnetic resonance imaging. *Aliment. Pharmacol. Ther.* **22**: 971–979
- Stopher, D. A., Beresford, A. P., Macrae, P. V., Humphrey, M. J. (1988) The metabolism and pharmacokinetics of amlodipine in humans and animals. *J. Cardiovasc. Pharmacol.* **12**: 55–59
- Vertzoni, M., Symillides, M., Iliadis, A., Nicolaides, E., Reppas, C. (2003) Comparison of cumulative drug vs. time data sets with indices. *Eur. J. Pharm. Biopharm.* **56**: 421–428
- Vertzoni, M., Fotaki, N., Kostewicz, E., Stippler, E., Leuner, C., Nicolaides, E., Dressman, J., Reppas, C. (2004) Dissolution media simulating the intraluminal composition of the small intestine: physiological issues and practical aspects. *J. Pharm. Pharmacol.* **56**: 453–462
- Vincent, J., Harris, S. I., Foulds, G., Dogolo, L., Willavize, S., Friedman, H. L. (2000) Lack of effect of grapefruit juice on the pharmacokinetics and pharmacodynamics of amlodipine. *Br. J. Clin. Pharmacol.* **50**: 455–463
- Wagner, J. G. (1993) *Pharmacokinetics for the pharmaceutical scientist*. Technomic Publishing Co. Inc., Basel.
- Yamashita, S., Furubayashi, T., Kataoka, M., Sakane, T., Sezaki, H., Tokuda, H. (2000) Optimized conditions for prediction of intestinal drug permeability using Caco-2 cells. *Eur. J. Pharm. Sci.* **10**: 195–204
- Yee, S. (1997) *In vitro* permeability across Caco-2 cells (colonic) can predict *in vivo* (small intestinal) absorption in man – fact or myth. *Pharm. Res.* **14**: 763–766
- Yoshida, F., Topliss, J. G. (2000) QSAR model for drug human oral bioavailability. *J. Med. Chem.* **43**: 2575–2585
- Yu, L. X. (1999) An integrated model for determining causes of poor oral drug absorption. *Pharm. Res.* **16**: 1883–1887
- Yu, L. X., Lipka, E., Crison, J. R., Amidon, G. L. (1996) Transport approaches to the biopharmaceutical design of oral drug delivery systems: prediction of intestinal absorption. *Adv. Drug Del. Rev.* **19**: 359–376
- Zhu, C., Jiang, L., Chen, T. M., Hwang, K. K. (2002) A comparative study of artificial membrane permeability assay for high throughput profiling of drug absorption potential. *Eur. J. Med. Chem.* **37**: 399–407